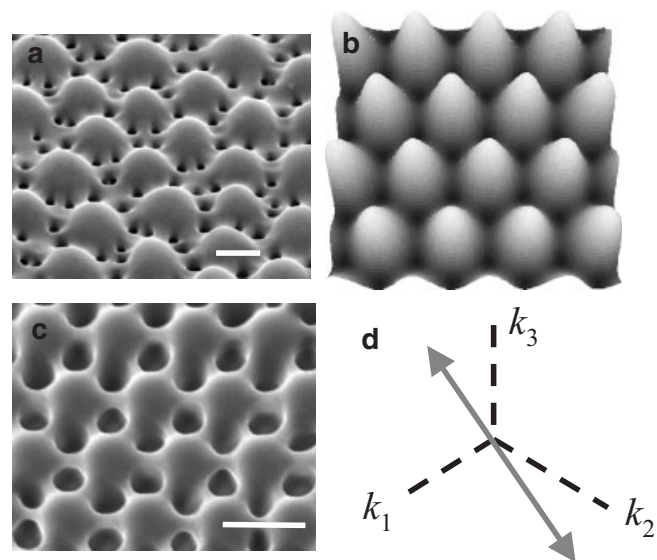


## Functional Biomimetic Microlens Arrays with Integrated Pores\*\*

By Shu Yang,\* Gang Chen, Mischa Megens, Chaitanya K. Ullal, Yong-Jin Han, Ronen Rapaport, Edwin L. Thomas, and Joanna Aizenberg\*

Biology provides a multitude of varied new paradigms for the development of adaptive optical networks.<sup>[1–7]</sup> Here, we present the first example of synthetic, biomimetic microlens arrays with integrated pores, whose appearance and function are strikingly similar to those of their biological prototype, a highly efficient optical element formed by brittlestars.<sup>[4]</sup> The complex microstructure is created directly by three-beam interference lithography in a single exposure. We show that i) the microlenses have strong focusing ability, and that ii) light-absorbing liquids can be transported in and out of the pores between the lenses, which provides the potential for a wide tunability range of the optical properties of the lens arrays.

We are interested in learning from natural optical systems, whose hierarchical architecture and hybrid character offer outstanding optical properties and enable multifaceted roles. Recently, we characterized a spectacular example of a biological, adaptive optical system—a close-set, nearly hexagonal array of uniform microlenses formed by the light-sensitive brittlestar, *Ophiocoma wendtii* (Fig. 1a).<sup>[4]</sup> The lenses were shown to be involved in photoreception, acting as optical elements that guide and concentrate light onto photosensitive tissue, and offering remarkable focusing ability, angular selectivity, and signal enhancement. An interesting design feature of this bio-optical structure is the presence of a pore network surrounding the lenses, which is essential to the diurnal migration of pigment-filled chromatophore cells.<sup>[8]</sup> Because of the



**Figure 1.** Structure of biological and biomimetic porous microlens arrays. a) Scanning electron microscopy (SEM) image of the design of a brittlestar lens. Scale bar: 50  $\mu\text{m}$ . b) Calculated light-intensity profile from three-beam interference lithography. Beam wavevectors and polarizations are described in the Experimental section. c) Corresponding SEM image of a synthetic, biomimetic microlens array with integrated pores. Scale bar: 5  $\mu\text{m}$ . d) Schematic drawing of the beam polarizations used (shown by double-headed arrow; viewed in the  $(0,0,\bar{1})$  direction) to realize the biomimetic lens shown in (c).

presence of a pore network, the brittlestar microlenses can be considered as an adaptive optical device that exhibits transmission tunability with a wide range, achieved by controlled transport of radiation-absorbing intracellular particles. The chromatocyte pigment also allows other functions, including diaphragm action, numerical-aperture tuneability, wavelength selectivity, minimization of the crosstalk between the lenses, and improved angular selectivity.

It is highly desirable to have small, complex photonic devices that can mimic the unusual design of the optical elements of the brittlestar and their consequent outstanding optical properties, by creating a structure that combines microlens arrays with the surrounding porous microfluidic system. The fabrication of such structures using existing techniques—ink-jet printing,<sup>[9]</sup> melting of patterned photoresists,<sup>[10]</sup> reactive ion etching of silica and silicon,<sup>[11]</sup> soft-lithography,<sup>[12]</sup> or self-assembly of monodispersed polymer beads<sup>[13]</sup>—is, however, not straightforward. Most of these techniques only create lenses without pore structures and their optical properties are not tunable. Multibeam interference lithography has been shown to be a fast, simple, and versatile method of creating two-dimensional (2D) and three-dimensional (3D) periodic, defect-free, porous microstructures over a large area.<sup>[14–18]</sup> The symmetry and the porosity of the resulting structures can be conveniently controlled by the wavevectors and polarizations of the interfering beams.<sup>[15,19]</sup> None of the previous studies, however, have either paid attention to the integration of the two different structures (lenses and pores) into a more

[\*] Prof. S. Yang  
Department of Materials Science and Engineering  
University of Pennsylvania  
3231 Walnut Street, Philadelphia, PA 19104 (USA)  
E-mail: shuyang@seas.upenn.edu

Dr. J. Aizenberg, Dr. G. Chen, Dr. Y.-J. Han, Dr. R. Rapaport  
Bell Laboratories, Lucent Technologies  
Murray Hill, NJ 07974 (USA)  
E-mail: jaizenberg@lucent.com

Dr. M. Megens  
Philips Research Laboratories  
Prof. Holstlaan 4, NL-5656 AA Eindhoven (The Netherlands)

C. K. Ullal, Prof. E. L. Thomas  
Department of Materials Science and Engineering  
Massachusetts Institute of Technology  
77 Massachusetts Ave, Cambridge, MA 02139 (USA)

[\*\*] The authors are grateful to A. Hale (OFS) for providing Irgacure 261 (Ciba Specialty Chemicals) in the experiments and helpful discussion of photosensitized holography in visible light. We acknowledge M. Li (Cornell) for discussion of microfluidics assemblies. The authors also thank their respective financial sources: Air Force DUR-INT in conjunction with the University of Buffalo (CKU), and ISN ARO (ELT).

complex photonic device, or shown resulting tunability of the optical properties of the lenses produced.

In our approach, we use three-beam interference lithography to create a synthetic, biomimetic analog of the brittlestar microlens array. Ours is the first example that combines both of the functional elements, the lenses and pores, in one structure. The geometry and polarizations of the laser beams were determined on the basis of theoretical calculations. We found that, while the wavevectors defined the translational symmetry of the structure, the polarization vectors were the key to the lens formation and its connectivity. For example, when the wavevectors were kept the same and the polarizations of the waves were parallel to each other (Fig. 1d), a periodic variation of light intensity with hexagonal symmetry was generated, and the simulated intensity profile resembled the shape of the biological lens array (Fig. 1b). In comparison, when the polarization of each wave was perpendicular to the difference between the other two wavevectors, we observed a threefold connectivity with a very small area of highest intensity, suggesting little or no lens formation (Fig. 2).

By subjecting a negative-tone photoresist, SU8, to the former interference light pattern, we have successfully created porous, hexagonal microlens arrays (Fig. 1c) that are markedly similar to their biological prototype (Fig. 1a). During exposure, the highly exposed regions of the photoresist cross-linked and became insoluble in an organic developer solution, while the unexposed or weakly exposed regions were dissolved away to reveal holes in the film. When the intensity difference between highly exposed and adjacent weakly exposed regions was above threshold, formation of a lens contour was

induced. The lens contour may have been amplified by factors such as the quantum efficiency of the photosensitive molecules (i.e., sensitizers and photoacid generators); the strong nonlinear relationship between the dose, polymerizability, and solubility change of the photoresists; as well as the shrinkage of the resist film during drying. We could control the lens size (diameter: 1.5–4.5  $\mu\text{m}$ ; height:  $\sim 200\text{ nm}$ –1.0  $\mu\text{m}$ ), shape, symmetry, and connectivity by adjusting the beam wavevectors and their polarizations, while the pore size and porosity were determined by the laser intensity and exposure time, respectively (porosity of about 10 to 80 %).

The ability of the thus-synthesized lens structures to focus light was studied using lithographic experiments, in which a film of a positive-tone photoresist, AZ5209, was illuminated through a synthetic lens array (Fig. 3a). When the illumination dose was fixed slightly below the sensitivity threshold of the photoresist ( $I_0$ ) to avoid exposure through the pores, the photoresist film appeared to be selectively exposed under each microlens because of their strong focusing activity. The pattern in the photoresist revealed hexagonally packed holes (Fig. 3b) that closely matched the microlens arrays seen in Figure 1c. The size of the features in the resist layer,  $a$ , could be effectively controlled by placing transparent spacers with different thicknesses,  $h$ , between the lens structure and the resist film (Fig. 3a). For example, for a lens diameter of  $\sim 4.1\ \mu\text{m}$ , the feature sizes in the photoresist gradually changed from  $\sim 3\ \mu\text{m}$  to  $\sim 700\text{ nm}$  near the focal point with  $h = 8\ \mu\text{m}$  (Fig. 3c). When the illumination dose was set above the lithographic threshold intensity, we observed one hole surrounded by six others under each lens, which originated from the pores in the lens arrays.

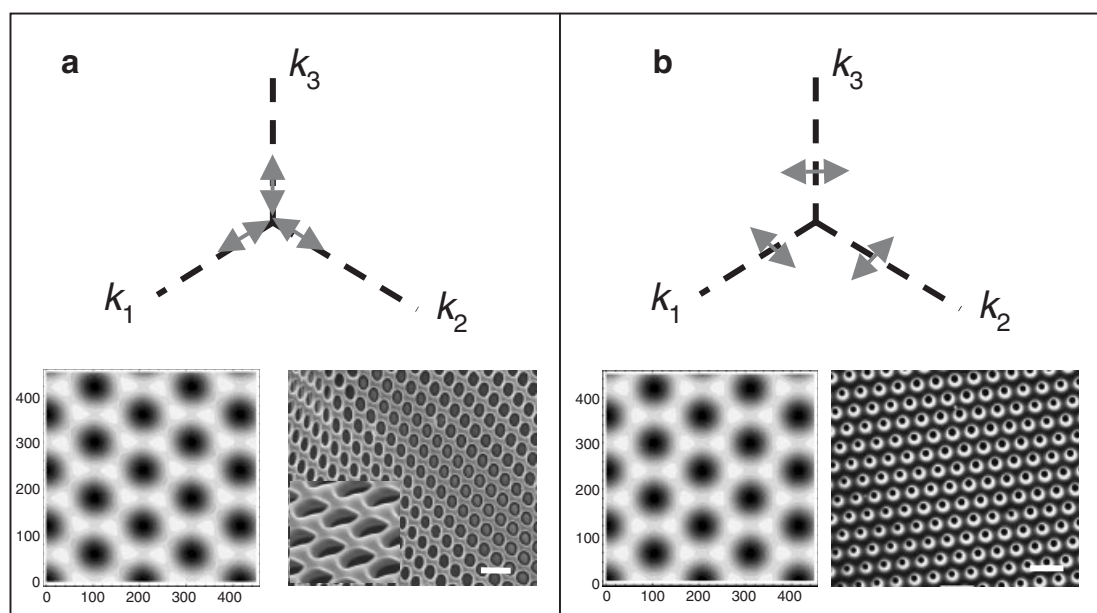


**Figure 2.** Formation of 2D structures in three-beam interference lithography using two different configurations of beam polarizations (shown by double-headed arrows) viewed in the  $(0,0,\bar{T})$  direction. In each panel, the left image shows the calculated total-intensity distribution using the consequent beam polarizations. The brightest region corresponds to the highest intensity of light. When calculating the intensity distribution for different beam polarizations, the change in polarization caused by reflection at the air/photoresist (SU8) interface was taken into account. The right image is the corresponding SEM image from the experiment. An enlarged SEM image is inserted in (a) to better demonstrate the lens. Scale bar: 5  $\mu\text{m}$ .

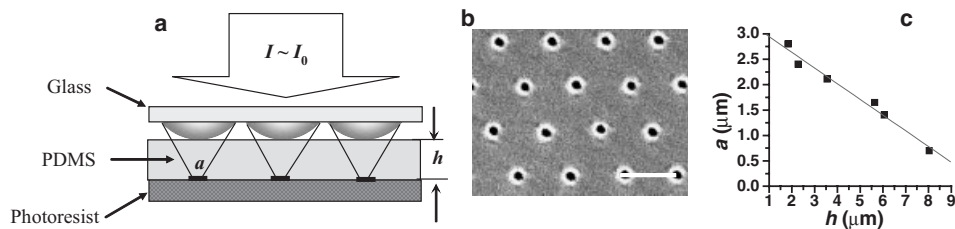


**Figure 3.** Focusing of light by the microlens array. a) Schematic representation of the experiment. b) SEM of features on a positive-tone photoresist exposed through the lens array near the focal point. Scale bar: 5  $\mu\text{m}$ . c) Dependence of the size of the produced features,  $a$ , on the distance between the array and the photoresist film,  $h$ .

Another application of the biomimetic microlens array is based on using the porous network as a microfluidic system that mimics pigment movement in the brittlestar stereom. We studied the possibility of actuating photoactive liquids within the microlens array. The thin film with the porous microlens arrays was assembled between two copper grids and a light-absorbing liquid was introduced from one side (see Experimental). When a dye-containing liquid was pumped through the pores (to mimic the migration of pigment-filled chromatophore cells in photosensitive brittlestars), the reduction in light transmission was detected under an optical microscope (Fig. 4). We observed a change of transmission ranging from 0 to 100 %, depending on the dye concentration and/or thickness of the dye layer covering the lens. This result clearly demonstrates that the presence of pore networks will allow the dynamic tuning of the optical properties of the lens. One potential application is as an optical shutter that turns light on and off in an optical interconnect. By using different liquids (e.g., liquids with varying refractive index and/or dyes that can

absorb at certain wavelengths) as the surrounding medium between the lenses, we can introduce further control over the lens focal length, numerical aperture, and wavelength selectivity.

Fabrication of microlens arrays with integrated pores, as reported here, is a first step toward creating and mimicking complex optical devices that are prominent in nature. The optical properties, tunability, and application of the synthetic structures presented clearly demonstrate that the lessons learned from sophisticated microlens arrays evolved by brittlestars for successful survival and adaptation may improve our current capabilities to construct new, microscale, adaptive optical devices that are potentially useful in a wide variety of technological applications. The knowledge we gain from fabricating these complex structures will provide important insights into creating novel, multifunctional, hybrid structures.

### Experimental

In the interference experiment, we used a continuous wave (CW) diode-pumped solid-state laser ( $\lambda = 532 \text{ nm}$ ) to photopolymerize SU8 (Shell Chemical). The primary laser beam was split into three beams which were overlapped onto a spot of diameter of 4–5 mm. For the lens structure shown in Figure 1, the wavevectors were arranged as:  $k_1 = 2\pi/a [0.035, 0, 0.999]$ ,  $k_2 = 2\pi/a [-0.017, 0.03, 0.999]$ ,  $k_3 = 2\pi/a [-0.017, -0.030, 0.999]$ . The polarizations of the waves were parallel. The resist was formulated by dissolving 2 wt.-% of Irgacure 261 (Ciba Specialty Chemicals), which acted as a photoacid generator sensitive to green light, and SU8 in cyclopentanone (~30–50 wt.-%). The solution was then spin-coated on a precleaned glass substrate, followed by soft baking at 90 °C to completely remove the solvent. The film thickness was in the range of 5–15  $\mu\text{m}$ , depending on the spin speed and resist concentration. When exposed to a laser beam (output of 2 W) for 1–6 s, photoacids were generated in the regions corresponding to the interference pattern. The ring-opening reactions of epoxy groups were initiated at a post-exposure bake and the acids were regenerated, resulting in a highly crosslinked film. Finally, the film was developed in propylene glycol methyl ether acetate (PGMEA) to remove unexposed or weakly exposed film, thus forming pores.

In the lithographic experiment that demonstrated the focusing ability of the synthetic microlens, a 1  $\mu\text{m}$  thick film of AZ5209 (Clariant International Ltd.) was spun on a glass substrate, followed by casting a polydimethylsiloxane (PDMS) film of varying thickness on top of the resist, to act as a transparent spacer. The lenses attached to a glass substrate were then placed directly on the PDMS spacer for conformal contact (Fig. 3a). First, we studied the minimum dose required to realize patterns (i.e., holes) in the resist. Then, we set the illumination dose just below the lithographic threshold and the photoresist was only exposed in the area where the beam was focused by the lenses.

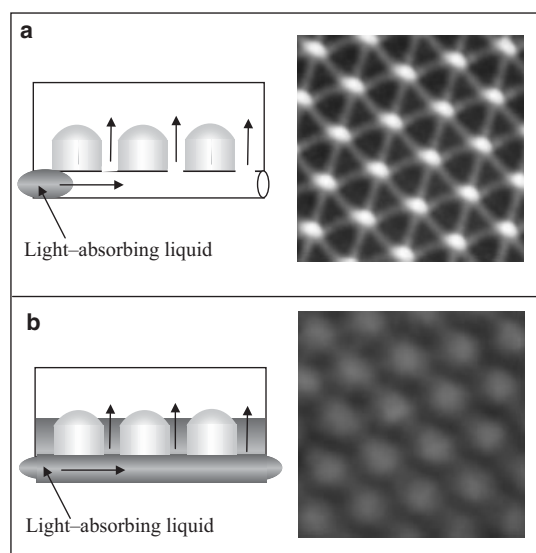


**Figure 4.** Illustration of the transmission tunability through the lens array, using controlled transport of a light-absorbing liquid in the channels between the lenses. Light micrographs were recorded in transmission mode near the focal point a) without, and b) with the light-absorbing liquid between the lenses.

For the microfluidics assembly, we sandwiched a film (3–4 mm in diameter) with lens arrays between two copper grids (3.05 mm diameter, 50 mesh) and sealed it with instant epoxy. We then carefully glued two micropipette tips on both sides of the copper grids and pumped a dye-containing liquid, e.g., water, tetrahydrofuran, or PGMEA, from one end using a syringe.

Received: June 25, 2004  
Final version: October 29, 2004

## Colloidal Crystal Capillary Columns— Towards Optical Chromatography\*\*

By Ulrich Kamp, Vladimir Kitaev,  
Georg von Freymann, Geoffrey A. Ozin,\*  
and Scott A. Mabury

Pressure-assisted colloidal-microsphere assembly in capillaries (PACMAC) is a novel technique that enables us to create monolithic colloidal-crystal capillary columns ( $C^c$ s) several centimeters long. Invariance of optical-diffraction spectra to rotation and translation over large length scales is demonstrated for these colloidal photonic crystals. PACMAC presents a fast, convenient, versatile, and robust synthetic approach to continuous polystyrene (PS) or silica capillary colloidal crystals with a wide range of microsphere and capillary diameters, which are shown to be suitable as templates for synthesizing inverse colloidal crystal capillary columns ( $IC^c$ s). Until now, capillaries have been completely filled with colloidal crystals by sedimentation, a process that requires weeks for completion.<sup>[1]</sup> Alternatively, colloidal crystal surface-coating films have been formed in capillaries, which requires meticulous control of the meniscus of the colloidal dispersion.<sup>[2]</sup> The micromolding-in-capillaries (MIMIC) technique has been used to confine the nucleation and growth of colloidal crystals to microchannels in a polydimethylsiloxane (PDMS) elastomeric stamp held in conformal contact with a planar substrate.<sup>[3]</sup>

In contrast to other colloidal-crystal formation methods, PACMAC does not occur at an dispersion–substrate interface by capillary forces<sup>[4]</sup> or by a sedimentation process.<sup>[1]</sup> The microsphere dispersion is forced into and through the capillary system of considerable length to the open end, and the resulting assembly exceeds the achievable length scales of other capillary techniques.<sup>[3]</sup> A colloidal-crystal plug or nucleation site is formed at the open capillary end by solvent evapora-

- [1] A. R. Parker, *J. Optics A-Pure Appl. Opt.* **2000**, *2*, R15.
- [2] A. R. Parker, V. L. Welch, D. Driver, N. Martini, *Nature* **2003**, *426*, 786.
- [3] M. F. Land, D.-E. Nilsson, *Animal Eyes*, Oxford University Press, New York **2002**.
- [4] J. Aizenberg, A. Tkachenko, S. Weiner, L. Addadi, G. Hendler, *Nature* **2001**, *412*, 819.
- [5] V. C. Sundar, A. D. Yablon, J. L. Grazul, M. Ilan, J. Aizenberg, *Nature* **2003**, *424*, 899.
- [6] P. Vukusic, J. R. Sambles, C. R. Lawrence, *Nature* **2000**, *404*, 457.
- [7] P. Vukusic, R. J. Wootton, J. R. Sambles, *Proc. R. Soc. London, Ser. B* **2004**, *271*, 595.
- [8] G. Hendler, M. Byrne, *Zoomorphology* **1987**, *107*, 261.
- [9] S. Biehl, R. Danzebrink, P. Oliveira, M. A. Aegerter, *J. Sol–Gel Sci. Technol.* **1998**, *13*, 177.
- [10] S. Haselbeck, H. Schreiber, J. Schwider, N. Streibl, *Opt. Eng.* **1993**, *32*, 1322.
- [11] P. Savander, *Opt. Lasers Eng.* **1994**, *20*, 97.
- [12] M. H. Wu, C. Park, G. M. Whitesides, *Langmuir* **2002**, *18*, 9312.
- [13] Y. Lu, Y. D. Yin, Y. N. Xia, *Adv. Mater.* **2001**, *13*, 34.
- [14] V. Berger, O. Gauthier Lafaye, E. Costard, *J. Appl. Phys.* **1997**, *82*, 60.
- [15] M. Campbell, D. N. Sharp, M. T. Harrison, R. G. Denning, A. J. Turberfield, *Nature* **2000**, *404*, 53.
- [16] I. B. Divliansky, A. Shishido, I. C. Khoo, T. S. Mayer, D. Pena, S. Nishimura, C. D. Keating, T. E. Mallouk, *Appl. Phys. Lett.* **2001**, *79*, 3392.
- [17] S. Yang, M. Megens, J. Aizenberg, P. Wiltzius, P. M. Chaikin, W. B. Russel, *Chem. Mater.* **2002**, *14*, 2831.
- [18] Y. V. Miklyaev, D. C. Meisel, A. Blanco, G. von Freymann, K. Busch, W. Koch, C. Enkrich, M. Deubel, M. Wegener, *Appl. Phys. Lett.* **2003**, *82*, 1284.
- [19] C. K. Ullal, M. Maldovan, M. Wohlgemuth, E. L. Thomas, C. A. White, S. Yang, *J. Opt. Soc. Am. A* **2003**, *20*, 948.

[\*] Prof. G. A. Ozin, U. Kamp, Dr. V. Kitaev,<sup>[+]</sup> Dr. G. von Freymann  
Materials Chemistry Research Group, Department of Chemistry  
University of Toronto  
80 Saint George Street, Toronto, Ontario, M5S 3H6 (Canada)  
E-mail: gozin@chem.utoronto.ca

U. Kamp, Prof. S. A. Mabury  
Environmental Chemistry, Department of Chemistry  
University of Toronto  
80 Saint George Street, Toronto, Ontario, M5S 3H6 (Canada)

Dr. G. von Freymann  
Institut für Nanotechnologie  
Forschungszentrum Karlsruhe in der Helmholtz-Gemeinschaft  
D-76021 Karlsruhe (Germany)

[+] Present address: Chemistry Department, Wilfrid Laurier University, 75  
University Avenue West, Waterloo, Ontario N2L 3C5, Canada.

[\*\*] GAO is Government of Canada Research Chair in Materials Chemistry. Financial support for this work from the University of Toronto and the Natural Sciences and Engineering Research Council of Canada is deeply appreciated. GvF acknowledges support through the Deutsche Forschungsgemeinschaft (DFG) under FR 1671/2-1.